

Ordered 1,6-bis(2-hydroxyphenyl) pyridine boron complex films grown on Ag(110): From submonolayer to multilayer

D. Y. Zhong,¹ F. Lin,¹ L. F. Chi,^{1,2,*} Y. Wang,² and H. Fuchs¹¹*Institute of Physics and Center for Nanotechnology (CeNTech), Universität Münster, Wilhelm-Klemm-Straße 10, 48149 Münster, Germany*²*Key Laboratory for Supramolecular Structure and Materials of Ministry of Education, College of Chemistry, Jilin University, 130012 Changchun, China*

(Received 17 November 2004; published 30 March 2005)

Ordered molecular films of a blue-light-emitting material, 1,6-bis(2-hydroxyphenyl) pyridine boron complex [(dppy)BF], grown on the Ag(110) surface by means of organic molecular beam epitaxy, were investigated by scanning tunneling microscopy (STM) and low-energy electron diffraction (LEED) under an ultrahigh vacuum. Two commensurate structures exist in the monolayer film grown at 300 K, as found by STM. In the monolayer film, two types of hydrogen bonds are formed between the molecules, which, in addition to the molecule-substrate interaction, essentially determine the monolayer structures. The structural evolution of the (dppy)BF films from submonolayer to three monolayers was monitored by LEED *in situ* and in real time. The results indicate that the growth of the first two monolayers is affected by the periodic potential on the substrate surface, while such a template effect is weakened beyond the second monolayer.

DOI: 10.1103/PhysRevB.71.125336

PACS number(s): 68.43.Fg, 81.15.Hi, 68.37.Ef, 61.14.Hg

I. INTRODUCTION

Organic semiconductors have become increasingly important for applications in optical and electronic devices.^{1,2} For the fabrication of devices such as organic thin-film transistors (OTFT's), the structure of organic films on different kinds of substrates, including metals, semiconductors, glass, and polymers, should be carefully controlled in order to improve the device performance. To date, organic molecular beam epitaxy (OMBE) is widely used to grow ordered organic films on crystalline surfaces.^{3,4} Due to the interaction between the organic molecules and the substrate, the spatially periodic potential on the substrate surface can usually act as a template for the growth of organic films, resulting in commensurate and/or point-on-line structures of ordered organic molecules, which is known as epitaxial-quasiepitaxial growth. Both the molecule-substrate and intermolecular interactions play important roles on the growth of the first monolayer (ML). The final structure of the epitaxial monolayer is energetically stable, resulting from the balance between molecule-substrate and intermolecular interactions. For most planar π -conjugated molecules, the influence of the molecule-substrate interaction will commonly extend to several layers during epitaxial growth. Further deposition of the organic molecules upon the first several layers leads to large stress in the film due to the mismatch between the surface-supported structure and the bulk one, resulting in the formation of islands.^{5,6} How to grow ordered multilayer films of organic semiconductors on a substrate is an open question both in basic research and in the fabrication of organic electronic and optical devices.

In epitaxial organic films, the van der Waals interaction and hydrogen bonds (H bond) are two major intermolecular interactions. In the case of growing π -conjugated molecules on noble metallic surfaces, the molecule-substrate interaction has the same order of magnitude as the intermolecular van

der Waals interaction. The H bond is a type of interactions that is much stronger than the van der Waals interaction.⁷ When H bonds are formed between the deposited molecule, the growth and molecular structure are modulated strongly by H bonds, in addition to the template effect of the substrate. Recently, much effort has been focused on the growth of H-bond-directed nanostructures on surfaces.⁸⁻¹¹ Barth *et al.* reported the formation of a one-dimensional superstructure of 4-[trans-2-(pyrid-4-yl-vinyl)]benzoic acid (PVBA) by self-assembly mediated by H bonds on a Ag(111) surface.⁸ Trimesic acid (TMA) is another typical molecule that can form H bonds. A two-dimensional honeycomb network induced by H bonds was obtained on Cu(100) surface.¹⁰ Furthermore, it was found that a more complex flower like structure of TMA molecules coexists with the honeycomb structure on the graphite surface.¹¹ Both of the superstructures are built based on the formation of H bonds between the molecules adsorbed on the surface.

In the present work, we investigate the growth of ordered monolayer and multilayer films of a blue-light-emitting organic semiconductor, 1,6-bis(2-hydroxyphenyl) pyridine boron complex [(dppy)BF],^{12,13} by OMBE. (dppy)BF is a non-planar molecule with one fluorine (F) and two oxygen (O) atoms, which are negatively charged. Both the F and O atoms tend to form H bonds with the hydrogen atoms from the neighboring molecules. Here, we discuss the effect of H bonds as well as the molecule-substrate interaction on the structure of the (dppy)BF monolayer grown on Ag(110). In order to understand the mechanism of multilayer growth of organic materials by OMBE, we investigated the structural evolution of (dppy)BF film from submonolayer to multilayer.

II. EXPERIMENT

The sample was prepared in an ultrahigh vacuum (UHV) with a background vacuum below 10^{-9} Torr. The Ag(110)

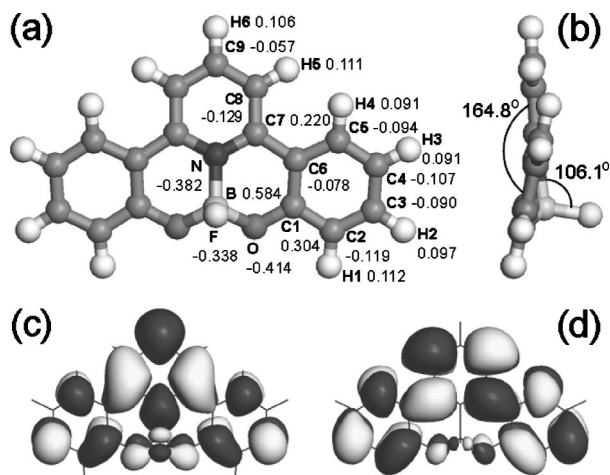


FIG. 1. Top view (a), side view (b), LUMO (c), and LUMO +1 (d) of isolated (dppy)BF molecule based on DFT calculation. The effective charge of atoms is labeled in (a).

surface was cleaned by a standard UHV process (sputtering by Ar^+ with beam energy of 500 eV for 15 min and then annealing at 800 K for 3 min). Before the growth of the (dppy)BF film, the organic material was degassed and purified in vacuum by heating to its sublimation temperature (380 K) and keeping this temperature for more than 3 h. The purified material was then sublimated onto the cleaned Ag(110) surface with a deposition rate of 0.25 ML/min. During the growth process, the vacuum in the chamber was about 2×10^{-9} Torr. The substrate was cooled down by liquid nitrogen, and the temperature on the substrate was measured by a Chromel-Alumel thermocouple located on the substrate holder. The growth process and structural evolution of the organic film was monitored in real time with a molecular-beam-epitaxy low-energy electron diffraction (MBE-LEED),¹⁴ on which three OMBE crucibles are integrated in order to record LEED patterns *in situ* during film growth. The monolayer films of (dppy)BF were investigated by an Omicron variable-temperature scanning tunneling microscope (VT-STM) in UHV at room temperature. Tungsten tips obtained by electrochemical etching were used for the STM experiments.

III. RESULTS

A. Geometrical structure of (dppy)BF

We have calculated the geometrical structure of an isolated (dppy)BF molecule by density functional theory (DFT). The calculation was carried out using a generalized-gradient-

corrected functional¹⁵ (PW91) with an energy convergence of 3×10^{-4} eV. Figures 1(a) and 1(b) give the top- and side-view model of the molecule after geometrical optimization. The molecule contains two benzene rings, one pyridine ring, and an sp^3 -hybrid boron (B) atom bound to fluorine (F), nitrogen (N), and oxygen (O) atoms. The DFT calculation indicates that the plane angle between the pyridine ring and the benzene rings is 164.8° . The F atom stands out from the main part of the molecule and the length of the F-B bond is 1.40 Å. The angle between the F-B and B-N bonds is 106.1° . The length of the molecule along the long axis is 14.06 Å. The calculated geometrical data of the isolated (dppy)BF molecule are listed in Table I. The experimental data, which were obtained from the x-ray diffraction of the (dppy)BF monoclinic crystal (symmetry group $P21/c$),¹⁶ is given for comparison.

The effective atomic charges calculated by DFT are labeled on each atom in Fig. 1(a). It is indicated that the negative charges are mainly located on the atoms of F (-0.338), O (-0.414), and N (-0.382), while B has the largest positive charge (0.584). Because of their large negative charges, F and O atoms tend to form H bonds with the H atoms from the neighboring molecules. In the case of the (dppy)BF monoclinic crystal, H bonds are formed between the F atoms and the H atoms on the benzene rings of the neighboring molecules.¹⁶ However, as discussed in the following sections, the (dppy)BF molecules deposited on Ag(110) are H bonded between the O atoms and the H atoms on the benzene and/or the pyridine rings of the neighboring molecules.

Furthermore, we calculated the molecular orbitals (MO's) of the (dppy)BF molecule. It was found that the highest occupied molecular orbital (HOMO) and the lowest unoccupied molecular orbital (LUMO) are located at -5.553 eV and -3.137 eV, respectively. The spatial distribution of the LUMO of the (dppy)BF molecule has an isosceles triangular shape, as is shown in Fig. 1(c), which is different from the spatial distribution of LUMO+1 (located at -2.892 eV) [Fig. 1(d)]. In the LUMO+1, the density is mainly distributed on the pyridine and benzene rings, and much less of the density is located at the F, O, and B atoms.

B. Monolayer structure grown at 300 K

The monolayer film of (dppy)BF was grown on Ag(110) surface at a temperature of 300 K. In order to adjust the thickness of the deposited films, we kept the sublimation temperature fixed at 380 K for each experiment so that the growth rate was invariable. The whole growth process was monitored by MBE-LEED and one monolayer was deposited on the substrate at the time when the diffraction pattern from

TABLE I. Geometrical data of an isolated (dppy)BF molecule compared with the result from a monoclinic crystal measured by x-ray diffraction.

	Molecule length	B-F	B-O	F-B-N	Benzene-pyridine plane angle
Theoretical (isolated)	14.06 Å	1.40 Å	1.46 Å	106.1°	164.8°
Experimental (monoclinic)	13.87 Å	1.42 Å	1.42 Å	104.8°	169.3°

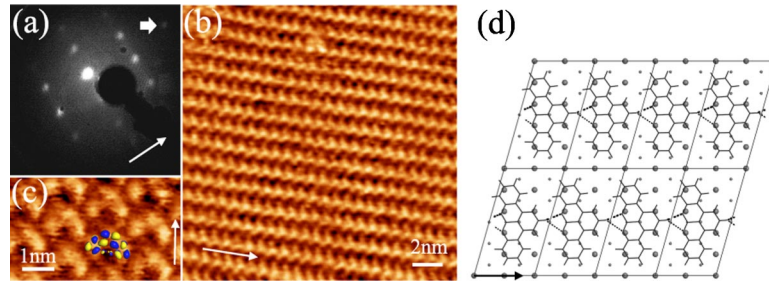


FIG. 2. (Color online). Structure $\alpha 5$ of (dppy)BF monolayer grown on Ag(110) at 300 K. (a) LEED pattern with beam energy of 13 eV. The thick arrow shows the (10) spot from Ag(110). (b) Constant current STM image, with $V_{\text{tip}} = -0.964$ V and $I = 0.19$ nA. (c) Constant-current STM image, with $V_{\text{tip}} = -1.222$ V and $I = 0.19$ nA. A LUMO+1 of (dppy)BF is drawn in the image. (d) Structural model of $\alpha 5$. H bonds are denoted by dotted lines. The thin arrows in (a)–(d) show the Ag[001] direction.

the sample was sharpest and brightest. In the present work, the growth time for one monolayer was 4 min. The structure of the as-grown monolayer was analyzed by LEED *in situ* and then checked by STM. Figure 2(a) is the LEED pattern of the (dppy)BF monolayer under an electron beam energy of 13 eV. The orientation of the Ag(110) substrate is denoted by a thin arrow on the image and the substrate (1 0) diffraction is denoted by a thick arrow at top-right corner of the image. The sharp diffraction spots indicate that a well-ordered organic monolayer was obtained. The diffraction pattern corresponds to one set of spots, indicating that the monolayer of (dppy)BF on the Ag(110) surface has only one periodic structure and one orientation domain. From the length and angle relationship between the reciprocal lattice vectors of the Ag(110) surface and those of the (dppy)BF monolayer, we calculate the transfer matrix of the real-space lattice vectors of the monolayer superstructure (denoted as $\alpha 5$) relative to the Ag(110) surface structure:

$$\begin{pmatrix} \mathbf{b}_1 \\ \mathbf{b}_2 \end{pmatrix}_{\alpha 5} = \begin{pmatrix} 2 & 0 \\ 1 & 5 \end{pmatrix} \begin{pmatrix} \mathbf{a}_1 \\ \mathbf{a}_2 \end{pmatrix},$$

where $\mathbf{b}_{1,2}$ and $\mathbf{a}_{1,2}$ are the base vectors of the monolayer superstructure and the Ag(110) surface ($a_1 = 4.086$ Å and a_2

$= 2.889$ Å), respectively. The angle between \mathbf{b}_1 and \mathbf{b}_2 and the angle between \mathbf{b}_1 and \mathbf{a}_1 are 74° and 0° , respectively. Each unit cell contains one molecule and the area per molecule is 1.18 nm². The geometrical parameters of structure $\alpha 5$ are listed in Table II.

The STM gives directly the real-space configuration of individual molecules and the periodic structure of the organic monolayer. Figure 2(b) shows the constant-current STM topography of (dppy)BF monolayer film grown on Ag(110) at 300 K. The voltage applied on the STM tip is $V_{\text{tip}} = -0.964$ V and the tunneling current is $I = 0.19$ nA. The orientation of the Ag(110) surface is denoted by a thin arrow in the image. A well-ordered periodic structure of the (dppy)BF monolayer was found in the STM image, in which the molecules are aligned one by one along the Ag [001] direction. We use the data from the STM to calculate the superstructure matrix and the structural parameters of the monolayer. The result is exactly the same as that obtained from LEED data.

The contrast of a constant current STM image corresponds to the local density of states (LDOS) as well as height fluctuation of the scanned surface. Figure 2(c) shows the submolecular-resolved STM image with a tip voltage of

TABLE II. Crystallographic data for the ordered structures of (dppy)BF grown on Ag(110). \mathbf{b}_1 and \mathbf{b}_2 are the base vectors of the superstructure; $\Phi(\mathbf{b}_1, \mathbf{b}_2)$ and $\Gamma(\mathbf{b}_1, \mathbf{a}_1)$ are the angles between \mathbf{b}_1 and \mathbf{b}_2 and between \mathbf{b}_1 and the Ag [001] direction, respectively. The number of molecules per unit cell (mol/cell) and the area per molecule (area/mol) are listed in the table. The data of the (100) plane of the (dppy)BF monoclinic crystal are present for comparison.

Structure	$\alpha 5$	β	$\gamma 5$	$\alpha 4.5$	$\gamma 9$	bulk (010)
Matrix	$\begin{pmatrix} 2 & 0 \\ 1 & 5 \end{pmatrix}$	$\begin{pmatrix} 3 & -4 \\ 2 & 6 \end{pmatrix}$	$\begin{pmatrix} 2 & 0 \\ 0 & 5 \end{pmatrix}$	$\begin{pmatrix} 2 & 0 \\ 1 & 4.5 \end{pmatrix}$	$\begin{pmatrix} 2 & 0 \\ 0 & 9 \end{pmatrix}$	
b_1 (nm)	0.817	1.685	0.817	0.817	0.817	0.755
b_2 (nm)	1.501	1.916	1.445	1.363	2.600	2.242
$\Phi(\mathbf{b}_1, \mathbf{b}_2)$	74.2°	108.1°	90.0°	72.6°	90.0°	98.2°
$\Gamma(\mathbf{b}_1, \mathbf{a}_1)$	0°	-43.3°	0°	0°	0°	
Mol/cell	1	3	1	1	1	2
Area/mol (nm ²)	1.18	1.02	1.18	1.06	2.12	0.84
Growth temperature	300 K	300 K	260 K	260 K	260 K	
Thickness	1 ML	1 ML	0.7 ML	1 & 2 ML	1.4 ML ^a	

^aStructure $\gamma 9$ only exists in the second (sub)monolayer

−1.222 V and a tunneling current of 0.19 nA. Each molecule in the image contains three high-contrast parts, corresponding to the high LDOS at the two benzene rings and the pyridine ring, while in the middle of the molecule (the site of B and F atoms), the contrast is dark. It is very similar to the spatial distribution of the LUMO+1 orbital, which is 0.245 eV higher than the LUMO [see Fig. 1(d)]. The LUMO+1 of (dppy)BF is drawn on Fig. 2(c) showing the relative spatial configuration of the molecules adsorbed on Ag(110).

At the same time, it was also found from the STM that the mirror axis of the (dppy)BF molecule, which is perpendicular to the long axis, deviates slightly from the Ag[001] direction of the surface, with a deviation angle less than 10°.

Most of the planar aromatic molecules—for example, pentacene, coronene, perylene, and their derivatives—are adsorbed on noble metals with their molecular plane parallel to the surface of the substrates. As for nonplanar molecules, there are more spatial configurations than for planar molecules. Chloro[subphthalocyaninato]boron(III) (SubPc) is a cone-shaped, nonplanar molecule with a central boron atom and an apex chlorine which is bound to a B atom. The growth of SubPc on Ag(111) was studied by Berner *et al.*¹⁷ Based on the chemical shift of the chlorine (Cl) 2*p* binding energy for submonolayer coverage measured by photoelectron spectroscopy, it was concluded that the SubPc molecule is adsorbed with its Cl atom towards the substrate. As discussed in Sec. III A, (dppy)BF is a nonplanar molecule, which contains two planar parts (two benzene rings and one pyridine ring), and an F atom standing out from the main part of the molecule. There are two possible adsorption states, with the F atom towards or away from the substrate. Due to the relatively strong interaction between halogen and the Ag substrate,¹⁷ it is supposed that the adsorbed (dppy)BF molecules lie on the Ag(110) surface with their F atoms towards the substrate, though no photoelectron spectroscopy data are available yet.

Based on the LEED and STM data described above, a real-space model is given in Fig. 2(d), showing the spatial configuration of the (dppy)BF monolayer relative to the Ag(110) surface. It is indicated in this model that the (dppy)BF molecules are aligned along Ag[001] direction. The mirror axis of each molecule deviates from the Ag [001] direction with a deviation angle of 3°. The distance between the apex hydrogen atom at the pyridine ring and the two oxygen atoms at one of its neighboring molecules is 2.3 and 2.7 Å, respectively. The H···O distance is small enough to form H bonds,⁷ which are denoted by dotted lines in Fig. 2(d).

Besides structure $\alpha 5$ of the monolayer (dppy)BF mentioned above, another structure (denoted as β) was found by STM, which is more complex than the structure $\alpha 5$, containing three molecules in each unit cell. Though both structures $\alpha 5$ and β coexist in the monolayer film, the latter has not been detected by LEED, probably because it is a minority phase in the monolayer film. Figure 3(a) shows the STM constant-current image of the structure with $V_{\text{tip}} = -0.567$ V and $I = 0.224$ nA. We also obtained the STM image in which both structure $\alpha 5$ and structure β were observed at the same time, which indicates that the structure β was not induced by

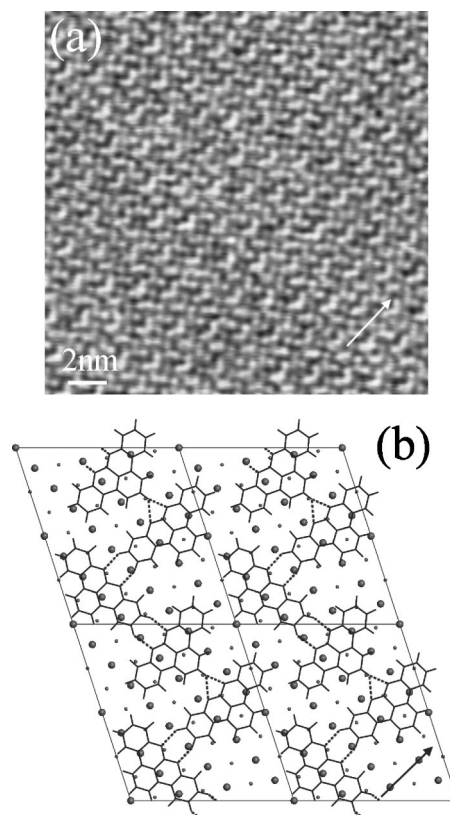


FIG. 3. Structure β of (dppy)BF monolayer grown on Ag(110) at 300 K. (a) Constant-current STM image, with $V_{\text{tip}} = -0.567$ V and $I = 0.19$ nA. (b) Structural model of β . H bonds are denoted by dotted lines. The thin arrows in (a) and (b) show the Ag[001] direction.

the STM tip during STM experiment. The real-space lattice relationship between the structure β and the Ag(110) substrate is calculated from the STM data:

$$\begin{pmatrix} \mathbf{b}_1 \\ \mathbf{b}_2 \end{pmatrix}_{\beta} = \begin{pmatrix} 3 & -4 \\ 2 & 6 \end{pmatrix} \begin{pmatrix} \mathbf{a}_1 \\ \mathbf{a}_2 \end{pmatrix}.$$

The angle between \mathbf{b}_1 and \mathbf{b}_2 and the angle between \mathbf{b}_1 and \mathbf{a}_1 are 74° and 0°, respectively. A model for this structure is shown in Fig. 3(b). One of the three molecules in a unit cell is adsorbed on Ag(110) with its mirror axis nearly parallel to the Ag[001] direction (called a type-I molecule), while the other two molecules are adsorbed with their mirror axis nearly perpendicular to the [001] direction (called a type-II molecule). The area per molecule in structure β is 1.02 nm², which is smaller than that of structure $\alpha 5$. The H bonds formed between two neighboring type-II molecules are similar to those formed in the former structure, while the H bonds between type-I and type-II molecules are very different. Two hydrogen atoms from the benzene ring at the type-II molecule were H bonded to two oxygen atoms from the neighboring type-I molecule. At the same time, two hydrogen atoms from the benzene ring at the type-I molecule H bonded to two oxygen atoms from another neighboring type-II molecule. The H bonds (C-H···O) are denoted by dotted lines in Fig. 3(b).

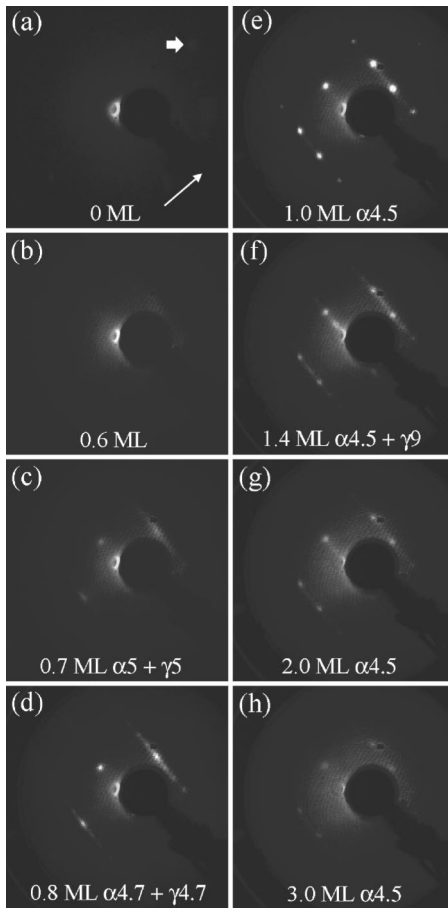


FIG. 4. LEED sequence shows the structural evolution of (dppy)BF film grown on Ag(110) at 260 K. Beam energy, 20 eV. (a) 0 ML. (b) 0.6 ML. (c) 0.7 ML. (d) 0.8 ML. (e) 1.0 ML. (f) 1.4 ML. (g) 2.0 ML. (h) 3.0 ML. The thick and thin arrows in (a) show the (01) spot and the [001] direction of Ag(110), respectively.

C. Structural evolution of (dppy) BF film grown at 260 K: From submonolayer to multilayer

The structure of the initial molecular layers is important for the further growth of organic films during epitaxial growth. In order to investigate the growth process of (dppy)BF film at the initial stage, an MBE-LEED was used *in situ* and in real time to monitor the structural evolution of the film.

Figure 4 shows a LEED sequence of a (dppy)BF film grown on Ag(110) at a substrate temperature of 260 K. The Ag[001] direction is denoted by the thin arrow in Fig. 4(a), and the nominal film thickness is given in each LEED image. An electron beam with energy of 20 eV was used during the whole experiment. Before the growth of the (dppy)BF film (0 ML), the substrate (0 1) diffraction spot appears in the LEED pattern (indicated by the thick arrow), as well as the bright (0 0) spot [Fig. 4(a)]. When the submonolayer film with a nominal thickness of 0.6 ML was grown on the substrate, a diffused squarelike pattern was found on the LEED screen, which indicates the nucleation of the disordered molecules deposited on the surface [Fig. 4(b)]. At a film thickness of 0.7 ML, separated spots were obtained in the LEED

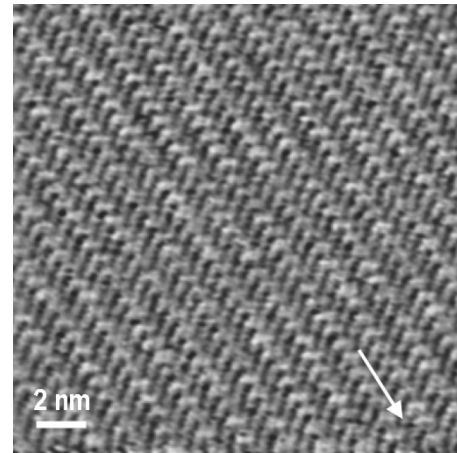


FIG. 5. Constant-current STM image of (dppy)BF monolayer grown on Ag(110) at 260 K, with $V_{\text{tip}} = -0.929$ V and $I = 0.2$ nA. The arrow shows the Ag[001] direction.

pattern, which corresponds to two periodic structures. One of them is structure $\alpha 5$, which has already appeared in the monolayer grown at 300 K, and the other one is a new structure denoted by $\gamma 5$, with its base vectors written as

$$\begin{pmatrix} \mathbf{b}_1 \\ \mathbf{b}_2 \end{pmatrix}_{\gamma 5} = \begin{pmatrix} 2 & 0 \\ 0 & 5 \end{pmatrix} \begin{pmatrix} \mathbf{a}_1 \\ \mathbf{a}_2 \end{pmatrix}.$$

Continuing deposition at a submonolayer stage resulted in the diffraction patterns of both structures being slightly expanded along the $[1\bar{1}0]$ direction, which indicates the real-space structures were compressed along $[1\bar{1}0]$ direction. Figure 4(d) shows the LEED pattern at 0.8 ML. The matrices for the compressed structures are

$$\begin{pmatrix} 2 & 0 \\ 0 & 4.7 \end{pmatrix} \quad \text{and} \quad \begin{pmatrix} 2 & 0 \\ 1 & 4.7 \end{pmatrix}$$

(denoted as $\gamma 4.7$ and $\alpha 4.7$), respectively. Increasing the film thickness after 0.8 ML leads to weakening of γ pattern and brightening of α pattern. Up to a monolayer film [Fig. 4(e)], the γ structure disappeared and a unique compressed α structure, $\alpha 4.5$, was obtained, which is described as

$$\begin{pmatrix} \mathbf{b}_1 \\ \mathbf{b}_2 \end{pmatrix}_{\alpha 4.5} = \begin{pmatrix} 2 & 0 \\ 1 & 4.5 \end{pmatrix} \begin{pmatrix} \mathbf{a}_1 \\ \mathbf{a}_2 \end{pmatrix}.$$

Figure 5 shows The STM image of the monolayer film grown on Ag(110) at 260 K. The experimental parameters are $V_{\text{tip}} = -0.929$ V and $I = 0.2$ nA. The configuration of the (dppy)BF molecules is very similar to the monolayer structure $\alpha 5$ grown at 300 K, except that the period along the Ag $[1\bar{1}0]$ direction is smaller than that of structure $\alpha 5$. The structural models of $\gamma 5$ and $\alpha 4.5$ are given in Figs. 6(a) and 6(b), respectively. Note that $\gamma 5$ is a commensurate structure but $\alpha 4.5$ is a point-on-line structure.

After the formation of the first monolayer on Ag(110), a second molecular layer was deposited on it. During the initial stage of the second monolayer growth, a transitional structure was formed first. Figure 4(f) shows the LEED pat-

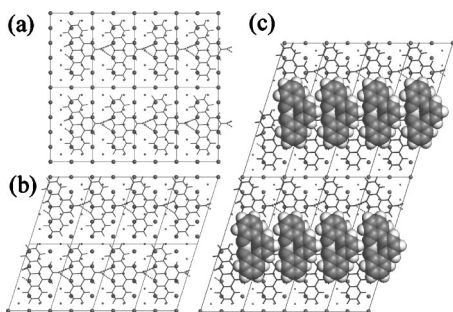


FIG. 6. Structural models of (dppy)BF grown on Ag(110) at 260 K. (a) Relaxed submonolayer structure γ_5 . (b) Structure $\alpha_{4.5}$ at 1.0, 2.0, and 3.0 ML. (c) Transitional structure γ_9 at 1.4 ML. H bonds are denoted by dotted lines in (a)–(c)

tern of the (dppy)BF film with a nominal thickness of 1.4 ML. Besides of the diffraction spots of the structure $\alpha_{4.5}$ from the first monolayer, there is another set of spots which result from the top submonolayer. The transitional structure, with the period along the $[1\bar{1}0]$ being twice of the underlying monolayer, corresponds to the following relationship (denoted as γ_9):

$$\begin{pmatrix} \mathbf{b}_1 \\ \mathbf{b}_2 \end{pmatrix}_{\gamma_9} = \begin{pmatrix} 2 & 0 \\ 0 & 9 \end{pmatrix} \begin{pmatrix} \mathbf{a}_1 \\ \mathbf{a}_2 \end{pmatrix}.$$

A structural model of γ_9 is proposed in Fig. 6(c). The molecules in this structure are bound to their neighboring molecules by H bonds and aligned one by one along the Ag[001] direction. The distance between the molecular rows is 9 times lattice period along the Ag $[1\bar{1}0]$ direction. The structure γ_9 is commensurate to the substrate, though the underlying monolayer is point on line. The result suggests that the growth of the second monolayer is affected not only by the underlying molecular monolayer but also by the surface periodicity of the metallic substrate.

The transitional structure γ_9 continuously decayed and ultimately disappeared when a second monolayer was grown on the Ag(110) surface [Fig. 4(g)]. The periodic structure of the second monolayer is the same as that of the first monolayer—i.e., structure $\alpha_{4.5}$. In other words, another molecular row was deposited and filled in the empty sites between the neighboring rows in structure γ_9 .

The periodic structure of the (dppy)BF film is almost invariant beyond the second monolayer, exhibiting structure $\alpha_{4.5}$. Figure 4(h) shows the LEED pattern at a thickness of 3 ML. The diffraction spots are weakened and the background is a little bright, compared with the LEED obtained at monolayer thickness. The result indicates that the multilayer film is partially disordered.

IV. DISCUSSION

The crystallographic data of the ordered structure of (dppy)BF grown on Ag(110) are listed in Table II. The five structures that we have obtained belong to three types: α , β , and γ . The molecules in type- α and γ structures lie on the surface with their mirror axis nearly parallel to the Ag[001]

direction. They are aligned one by one along the Ag[001] direction, bound to two neighboring molecules by H bonds. In the α -type structures, molecules between the neighboring rows are staggered along the Ag $[1\bar{1}0]$ direction, which is different from the type- γ structures, in which molecules between the neighboring rows are side by side. Only van der Waals interactions exist between the neighboring molecules along the Ag $[1\bar{1}0]$ direction. Since the H bonds are much stronger than the van der Waals interactions, both type- α and γ structures are energetically stable. In α and γ structures, there is one molecule in a unit cell, while structure β contains three molecules in a unit cell. Two of them are adsorbed with their mirror axis nearly parallel to the Ag[001] direction; the other one with its mirror axis nearly perpendicular to the Ag[001] direction. The occupied area per molecule in structure β is 1.02 nm^2 , which is even smaller than the value (1.06 nm^2) for the compressed structure $\alpha_{4.5}$. The occupied areas per molecule in all the surface-supported structures are greater than that (0.84 nm^2) in the (010) plane in the (dppy)BF monoclinic crystal.

It is known that the structure of organic thin films grown by OMBE is determined by both the intermolecular and the molecule-substrate interactions. At a submonolayer stage, the molecules are relaxed on Ag surface and organized in the commensurate structures (α_5 and γ_5), so that the adsorption energy is minimized. When more molecules are deposited on the surface, the distance between the molecules along Ag $[1\bar{1}0]$ is reduced continuously and at last a compressed structure $\alpha_{4.5}$ is formed at nearly one monolayer coverage. Note that only the distance along Ag $[1\bar{1}0]$ is reduced, while the distance along Ag[001] is invariant. The reason is that the van der Waals energy is changed slowly when the molecule-molecule distance is changed, while the binding energy of H bonds is affected by bond length critically. The structure compression has been also found for 2,5-dimethyl-dicyanoquinonediimine films grown on Ag(110), as reported by Seidel *et al.*¹⁸ The structure evolution at the submonolayer stage indicates that the molecules have a large mobility on the Ag(110) surface.

As is described in Sec. III A, the F and O atoms of the (dppy)BF molecule have a partial negative charge. It is possible to form H bonds between F, O, atoms and H atoms from the benzene and pyridine rings. In a monoclinic crystal, the H bonds are formed between F and H atoms on the benzene ring of the molecule from the neighboring (010) plane.¹⁶ The case of surface-supported monolayer structure is completely different because the molecules in a monolayer are parallel to each other and the F atoms are far away from the H atoms. Only O atoms contribute to the H-bond formation. There are two types of H-bond configurations. One is formed between both O atoms of one molecule and the apex H atom on the pyridine ring of the other molecule (type I); the other type is formed between the two O atoms of one molecule and the two H atoms on the same benzene ring of the other molecule (type II). The lengths of type-I H bonds are 2.3 and 2.7 Å, which exist in α and γ structures [see Figs. 2(d), 5(a), and 5(b)]. Note that the two C-H \cdots O bonds are different due to the deviation between the (dppy)BF mir-

ror axis and the Ag[001] direction. In structure β , there are two type-I and four type-II H bonds in a unit cell [see Fig. 3(b)]. In other words, each molecule is bound to others by four H bonds. The length of type-II H bonds in structure β is in the range of 2.3–2.8 Å.

Since the (dppy)BF molecules easily diffuse on the Ag(110) surface at 300 K and even at 260 K, at the initial stage (before 0.7 ML), the molecules deposited on the surface are disordered, moving randomly on the surface. The H bond can be formed when two molecules collide with each other. The H-bonded molecules lose their mobility on the substrate surface and act as nucleation centers. More molecules join in and finally an ordered film is formed.

The first monolayer of (dppy)BF grown at 260 K has an point-on-line structure ($\alpha 4.5$). When growing the second monolayer, a commensurate structure $\gamma 9$ was formed at the submonolayer stage. This result indicates that there is a considerable interaction between the substrate and the molecules in the second layer, so that the substrate template effect still persists during the growth of the second monolayer. After the second layer, the molecule-substrate interaction is weakened enough so that the effect of intermolecular interaction, compared to the molecule-substrate interaction, is enhanced in the growth beyond the second layer. The third layer is disordered to some extent, because the multilayer growth beyond the second monolayer tends to follow the bulk crystalline structure rather than the surface-supported structure, which is affected by the surface potential of the substrate. Similar to the (010) plane of (dppy)BF monoclinic crystals, in which a half number of molecules are orientated with their F atoms upward and the other half number of molecules downward, the molecules beyond the second monolayer in the OMBE film have probabilities being orientated with their F atoms both upward and downward, due to the interlayer interactions between the molecules.

The present result is consistent with the growth of 3,4,9,10-perylene-tetracarboxylic dianhydride (PTCDA) on Au(111) and Ag(111) surfaces^{19,20} and tin phthalocyanine (SnPc) on the sulphur-terminated GaAs(001) surface.²¹ In the high-temperature (equilibrium) growth region, the growth of the first two monolayers of PTCDA on Au(111) is layer-by-layer mode, while the film acquires a three-dimensional morphology beyond 2 ML.¹⁹ SnPc is one kind of nonplanar molecules with the central metal atom lying above the plane of the molecule. The SnPc films grown on sulphur-terminated GaAs(001) surface follow a Stranski-Krastanov growth mode, involving layer-by-layer epitaxy for the first few layers and then island formation beyond a film thickness of around 12 Å.²¹

V. CONCLUSION

Ordered monolayer films of (dppy)BF, a blue-light-emitting, nonplanar molecule, was obtained by OMBE. Two

structures, $\alpha 5$ and β , were found in the film. Both structures are stabilized mainly by H bonds between the adsorbed molecules. Two types of H bonds exist in the monolayer film. The type-I H bond is formed between the two O atoms of the (dppy)BF molecule and the apex H atom from the pyridine ring of the neighboring molecule. The molecules bound by type-I H bonds are nearly parallel to each other. The type-II H bond is formed between the two O atoms and two H atoms from the benzene ring of the neighboring molecule. The molecules bound by type-II H bonds are perpendicular to each other. Due to the confinement of the substrate surface, the configuration of H bonds formed in the surface-supported structure is very different from that formed in the bulk molecular crystal, in which H bonds are formed between F atoms and H atoms from the benzene ring. In structure $\alpha 5$, the molecules are bound by type-I H bonds and aligned one by one along the Ag[001] direction. Structure β is more complex and contains three molecules per unit cell, which are bound by both type-I and -II H bonds.

The STM contrast of (dppy)BF with $V_{\text{tip}} = -1.222$ V shows high LDOS at the two benzene rings and the pyridine ring and low LDOS in the middle of the molecule (the site of B and F atoms). Compared to the MO's of (dppy)BF, it is concluded that the STM contrast corresponds to the density distribution of the LUMO+1 orbital, which is 0.245 eV higher than the LUMO.

The structural evolution of the (dppy)BF film from submonolayer to 3 ML was monitored by LEED *in situ* and in real time during the growth process. Two relaxed structures ($\alpha 5$ and $\gamma 5$) coexist at the submonolayer stage (0.7 ML). Both of them are compressed along the Ag[1 $\bar{1}$ 0] direction when increasing their coverage. At monolayer coverage, the γ structure disappears and a compressed structure $\alpha 4.5$ is formed. A transitional structure $\gamma 9$ is formed first at the submonolayer stage of the second monolayer, indicating the template effect of the substrate. Beyond the second monolayer, the substrate effect on the film growth is weakened. The ultimate structure of the second and third monolayers is $\alpha 4.5$, the same as the first monolayer. Our results help to understand the initial epitaxial growth of the multilayer organic film.

ACKNOWLEDGMENTS

The authors would like to thank Dr. C. Seidel, R. Arends, and S. Frie for their help in the experimental facility. This work was financially supported by the "Ministerium für Wissenschaft und Forschung" of North Rhine-Westphalia (NRW), the National Natural Science Foundation of China (Grant No. 50225313), and the Major State Basic Research Development Program (Grant No. 2002CB613401). The STM data were processed by the software WSxM 4.0 Develop 6.1 (Nanotec Electronica S.L.).

*Electronic address: chi@uni-muenster.de

- ¹B. Crone, A. Dodabalapur, Y.-Y. Lin, R. W. Filas, Z. Bao, A. LaDuca, R. Sarpeshkar, H. E. Katz, and W. Li, *Nature (London)* **403**, 521 (2000).
- ²C. D. Dimitrakopoulos and P. R. L. Malenfant, *Adv. Mater. (Weinheim, Ger.)* **14**, 99 (2002).
- ³M. Eremtchenko, J. A. Schaefer, and F. S. Tautz, *Nature (London)* **425**, 602 (2003).
- ⁴S. R. Forrest, *Chem. Rev. (Washington, D.C.)* **97**, 1793 (1997).
- ⁵A. C. Dürr, F. Schreiber, K. A. Ritley, V. Kruppa, J. Krug, H. Dosch, and B. Struth, *Phys. Rev. Lett.* **90**, 016104 (2003).
- ⁶F. Schreiber, *Phys. Status Solidi A* **201**, 1037 (2004).
- ⁷T. Steiner, *Angew. Chem., Int. Ed.* **41**, 48 (2002).
- ⁸J. V. Barth, J. Weckesser, C. Cai, P. Günter, L. Bürgi, O. Jeandupeux, and K. Kern, *Angew. Chem., Int. Ed.* **39**, 1230 (2000).
- ⁹J. A. Theobald, N. S. Oxtoby, M. A. Phillips, N. R. Champness, and P. H. Beton, *Nature (London)* **424**, 1029 (2003).
- ¹⁰A. Dmitriev, N. Lin, J. Weckesser, J. V. Barth, and K. Kern, *J. Phys. Chem. B* **106**, 6907 (2002).
- ¹¹S. Griessl, M. Lackinger, M. Edelwirth, M. Hietschold, and W. M. Heckl, *Single Mol.* **3**, 25 (2002).
- ¹²Y. Li, Y. Liu, W. Bu, J. Guo, and Y. Wang, *Chem. Commun. (Cambridge)* **2000**, 1551.
- ¹³J. Feng, F. Li, W. Gao, S. Liu, Y. Liu, and Y. Wang, *Appl. Phys. Lett.* **78**, 3947 (2001).
- ¹⁴C. Seidel, J. Poppensieker, and H. Fuchs, *Surf. Sci.* **408**, 223 (1998).
- ¹⁵J. P. Perdew and Y. Wang, *Phys. Rev. B* **45**, 13 244 (1992).
- ¹⁶Y. Wang *et al.* (unpublished).
- ¹⁷S. Berner, M. de Wild, L. Ramoino, S. Ivan, A. Baratoff, H.-J. Güntherodt, H. Suzuki, D. Schlettwein, and T. A. Jung, *Phys. Rev. B* **68**, 115410 (2003).
- ¹⁸C. Seidel, H. Kopf, and H. Fuchs, *Phys. Rev. B* **60**, 14 341 (1999).
- ¹⁹P. Fenter, F. Schreiber, L. Zhou, P. Eisenberger, and S. R. Forrest, *Phys. Rev. B* **56**, 3046 (1997).
- ²⁰B. Krause, F. Schreiber, H. Dosch, A. Pimpinelli, and O. H. Seeck, *Europhys. Lett.* **65**, 372 (2004).
- ²¹A. R. Vearey-Roberts, H. J. Steiner, S. Evans, I. Cerrillo, J. Mendez, G. Cabailh, S. O'Brien, J. W. Wells, I. T. McGovern, and D. A. Evans, *Appl. Surf. Sci.* **234**, 131 (2004).